Mathematical Modelling of Engineering Problems
Vol. 12, No. 2, February, 2025, pp. 523-532
Journal homepage: http://iieta.org/journals/mmep

Effects of Hydrolytic Aging on the Properties of Oil-Impregnated Pressboard

Mohammed Nedjar*, Fatima Kerkarine

Laboratoire de Génie Electrique, Université Mouloud Mammeri, Tizi-Ouzou 15000, Algeria

Corresponding Author Email: mohammed.nedjar@ummto.dz

https://doi.org/10.18280/mmep.120217

Received: 28 November 2024
Revised: 15 January 2025
Accepted: 20 January 2025
Available online: 28 February 2025

Keywords:
oil-impregnated pressboard, hydrolytic aging, dielectric strength, elongation at break, tensile strength, Weibull statistic, TGA, FTIR

ABSTRACT

Oil-impregnated pressboard is used in power transformers because of its excellent properties. This work aims to study the effects of hydrolytic aging on the properties of oil-impregnated pressboard. Circular samples and dumbbell form specimens were put in a climatic chamber regulated at 93% relative moisture and 40°C. The aging was achieved until 9500 h. Failure is a random phenomenon. Therefore, the values of the properties were analysed using the Weibull model. Scale parameters, shape parameters, and equations of curves were determined. The insulation was typified by TGA and FTIR. TGA represents the variation of mass versus temperature. FTIR depicts transmittance variation against wavenumber. These methods allow deducting the degradation. The investigation shows a change in dielectric strength, elongation at break, and tensile strength versus aging time. TGA curves exhibit modifications of the onset and the residue of degradation. FTIR findings highlight changes in the intensities of the absorbance peaks at 3344, 2917, and 1044 cm^{-1}. Extinction of the absorbance peak at 1653 cm^{-1} is noticed. The degradation was characterized by the formation of both 2-furfuraldehyde and dissolved carbon dioxide (CO_2) in the oil. The decomposition is governed by H+ ions resulting in the dissociation of carboxyl acids in water.

1. INTRODUCTION

High-voltage transformers are the essential and expensive equipment of electrical networks. Oil-impregnated pressboard is used in power transformers because of its advantages as high tensile strength, low shrinkage, high apparent density, and excellent insulating properties as yielded by Gao et al. [1].

Pressboard contains about 90% cellulose, 6-7% hemicellulose, and 3-4% lignin. For its realization, a quantity of 35 layers per mm of cellulose was pressed.

Cellulose is hygroscopic, namely, it can absorb water vapor from the environment. Oommen and Prevost [2] mentioned that, at room temperature, cellulose can hold from 4 to 8% moisture in the relative humidity between 30% and 70% on the manufactory ground. Therefore, it is useful to dry the transformers during the making process. The moisture level in the pressboard of a new power transformer should be about 0.5%.

Cellulose is composed of wood fibers and between them remains some air spaces: capillaries. Although the spaces are very small, they occupy a considerable volume as indicated by Dai and Wang [3]. Consequently, after drying, the pressboard must be impregnated by insulating oil. The process consists of filling the capillaries with oil which acts both as electrical insulation and thermal coolant. After impregnation, it is important to ensure that no cavities are left within the pressboard. The presence of the cavities can be the seat of partial discharges (PD) which could increase the rate of degradation.

The effects of moisture on the electrical properties of oil-impregnated pressboard were presented by several researchers [4-6]. Wen et al. [4] pointed out that breakdown voltage decreases versus moisture content. For a water amount of 0.98%, the value of breakdown voltage is 46.3 kV. While for a 5.02% moisture quantity, its value is 42.5 kV. Vahidi et al. [5] reported the rise of electrical conductivity of impregnated pressboard with moisture amount. For the tests, the values of the applied electric field are 0.5, 1.0, and 3.0 kV/mm. The increase of the moisture content in both oil and paper could lead to the rise of dielectric losses, and the shortening of insulation resistivity, and breakdown voltage as displayed by Wang et al. [6]. This process will have a significant negative effect on the oil-pressboard insulating property. Emsley and Stevens [7] exhibited that the lifetime of paper insulation weakens from 40 years to around 5 years when the moisture amount increases by 2% at 90°C.

Despite the good properties of oil-impregnated pressboard, researchers highlighted the degradation of the insulation under the action of moisture and temperature [8-10]. Jadav et al. [8] examined the effect of moisture and aging on the oil - impregnated pressboard properties. Samples of different moisture amounts were aged at 105°C until 1944 h. The authors found a change in moisture quantity in oil and pressboard during aging time. The content reached 7.4% and 74% for the pressboard and the oil, respectively. The authors mentioned about 80% reduction in polymerization degree. The researchers reported that the acidity in oil increases with aging time. The raise reached 0.11 mg KOH/g after 1944 h.

Khawaja et al. [9] investigated the partial discharge behaviour at high temperatures, between 80°C and 145°C, with different levels of moisture contaminations of both oil and pressboard. After a few days, it was noted that the presence of moisture reduces the dielectric strength of the material. Also, it was observed that the maximum PD level was lowered. Kumar and Haque [10] studied the dielectric properties of natural ester-impregnated pressboard under aging and moisture. The authors concluded a lessening of the insulation resistivity and an increase in dielectric loss factor versus aging time.

The goal of this investigation is to study dielectric strength, elongation at break, and tensile strength of oil-impregnated pressboard submitted to hydrolytic aging. The obtained data will be treated statistically by the Weibull model because mechanical failure and dielectric breakdown occur randomly. The Weibull statistic supplies information concerning the size distribution of defects. To study the degradation of the material, we use thermogravimetric analysis (TGA) and Fourier transform infrared spectroscopy (FTIR), which are widely employed to characterize polymers. TGA indicates the variation of the polymer mass versus temperature. The curves obtained before aging will be confronted by those after aging. FTIR exhibits the modification of transmittance (%) versus wavenumber(cm^{-1}). The spectra of the virgin samples will be compared to those of aged specimens.

2. EXPERIMENTAL TECHNIQUES

2.1 Sample preparation

Sheets of pressboard 2,000 mm × 1,000 mm × 1 mm were provided by ISOVOLTA, a Spanish manufacturer. The insulation is of class A 105°C.

For the tests of dielectric breakdown, a large number of circular samples having 75 mm in diameter was realized. For the mechanical tests, a great population of specimens, in dumbbell shape of 75 mm in length, was cut according to IEC 540 [11]. In order to shun the presence of defects, the samples were ascertained with a microscope.

The specimens were first dried in a ventilated air oven for 48 h at 105°C. Then mineral oil ("BORAK 22"), destined for impregnation, was dried under the same conditions. Afterward, the samples were put into an impregnation chamber at a vacuum level of 1 mbar for 72 h at 80°C.

2.2 Hydrolytic aging

After impregnation, the samples were quickly introduced in a climatic chamber regulated at 93% relative humidity and 40°C. The choice of these parameters is justified by the fact that high-voltage transformers are planned to be installed at an average temperature of 40°C under a medium relative humidity between 90% and 95%. To gain this moisture amount, 1.215 l of glycerin was mixed with 6.075 l of distilled water. The glycerin volume represents 20% of that of distilled water. The enclosure is equipped with a temperature regulator and a warming system. The aging was executed up to 9500 h (396 days).

2.3 Dielectric testing

After every 500 h of aging, 50 specimens were withdrawn from the climatic chamber. For the breakdown experiments, we used a cell outfitted by two circular plane electrodes made by stainless steel. To evade bypasses, the tank was filled by mineral oil of BORAK 22 type. Firstly, the sample was inserted between the electrodes. After, AC voltage ramp, supplied by high voltage transformer, was applied to the specimen until the breakdown occurred. The speed of voltage ramp is 0.5 kV/s. The tests were carried out at room temperature. After failure, the value of breakdown voltage was recorded and the thickness at rupture point was measured. The dielectric strength was calculated as the quotient of breakdown voltage to the thickness of the insulation at the failure point.

2.4 Mechanical testing

As the case of dielectric strength, after every 500 h, a sampling of 50 samples was taken from the climatic chamber. Before the test, the width and the thickness were measured at the middle of sample. The mechanical test consists of breaking the specimen under a tensile using a dynamometer with a velocity of 300 mm/min. The percentage of elongation at rupture, and the force at break were registered. The experiments were performed at ambient temperature. The tensile strength was defined as the ratio of the force at rupture to the section of the sample.

2.5 Characterization techniques

2.5.1 TGA

The TGA was performed with NETZSCH STA 409 PC/PG at temperatures locating between 25 to 800°C under nitrogen atmosphere. A little quantity of the oil-impregnated pressboard was deducted and placed in the crucible of the device micro-balance. The heating speed is 10°C/min and programmed with a computer. The average mass of the taken quantity is about 15 mg.

2.5.2 FTIR

For the realisation of the infrared spectra, a powder of the insulation was mixed with potassium bromide amount (KBr). After blending, the whole was pressed, and then the pellets were realized. The spectra were carried out with JASCO FT/IR equipment in wavenumber between 4000 and 400 cm^{-1}. The apparatus is connected to a computer.

3. STATISTICAL ANALYSIS

It is well known that mechanical failure is a random phenomenon described by Weibull model [12]. This statistical model is justified as soon as an anomaly detected at a microscopic level affects the entire system. This is the case in dielectric breakdown where a failure, originating in a very small volume of insulation, causes the entire rupture of the material. This model is widely applied in the study of dielectric breakdown of polymers [13-15]. In this work, the values of dielectric strength, elongation at break and tensile strength were analyzed statistically using Weibull model. The two-parameter Weibull distribution law is given by [16]:

$$P(X)=1-\exp\left[-\left(\frac{X}{X_0}\right)^{\beta}\right] \quad (1)$$

where,

P(X): cumulative failure probability.

X: random variable which may be, in this investigation, dielectric strength, elongation at break, and tensile strength.

X_0: scale parameter that is the value of X corresponding to a cumulative probability of 63.2%.

β: shape parameter which is the slope of the straight line of the Weibull plot.

The cumulative breakdown probability P was assessed using the following expression [17]:

$$P = \frac{i}{N+1} \times 100\% \quad (2)$$

where,

i: rank of data after a classification by ascending order.

N: total number of tested samples; in this study N = 50.

The various stages of statistical analysis were pointed out in a previous work [14]. Only the Weibull graphs corresponding to before aging and after 6000 h are exhibited for all the properties. The 90% confidence intervals are drawn by dash lines.

4. RESULTS AND DISCUSSION

4.1 Dielectric strength

4.1.1 Weibull graphs

Tables 1-3 show the statistical results of dielectric strength (E). Figure 1 displays the Weibull curves of E before aging and after 6000 h.

Table 1. Values of E and confidence intervals

Aging Time (h)	Dielectric Strength (kV)
0	46.716 < E = 47.737 < 48.726
500	35.822 < E = 37.467 < 39.097
1000	8.445 < E = 9.542 < 10.714
1500	7.209 < E = 8.152 < 9.160
2000	11.990 < E = 13.457 < 15.014
2500	26.620 < E = 28.015 < 29.405
3000	24.916 < E = 25.846 < 26.760
3500	23.890 < E = 24.877 < 25.851
4000	29.908 < E = 31.287 < 32.654
4500	27.876 < E = 29.114 < 30.339
5000	6.129 < E = 7.192 < 8.370
5500	23.565 < E = 24.589 < 25.601
6000	23.939 < E = 24.499 < 25.043
6500	26.489 < E = 27.570 < 28.635
7000	24.447 < E = 25.075 < 25.685
7500	24.745 < E = 25.387 < 26.011
8000	12.680 < E = 14.800 < 17.136
8500	23.501< E = 24.105<24.692
9000	13.978 < E = 16.165 < 18.554
9500	23.360 < E = 24.663 < 25.966

Table 2. Equation of Weibull plots

Aging Time (h)	Equation of Weibull Plot
0	Y = 11.985 X – 20.121
500	Y = 5.769 X – 9.079
1000	Y = 2.121 X – 2.078
1500	Y = 2.108 X – 1.921
2000	Y = 2.244 X – 2.533
2500	Y = 5.074 X – 7.344
3000	Y = 7.070 X – 9.985
3500	Y = 6.397 X – 8.929
4000	Y = 5.746 X – 8.592
4500	Y = 5.960 X – 8.727
5000	Y = 1.620 X – 1.388
5500	Y = 6.090 X – 8.469
6000	Y = 11.195 X – 15.552
6500	Y = 6.479 X – 9.333
7000	Y = 10.221 X – 14.302
7500	Y = 10.118 X – 14.212
8000	Y = 1.676 X – 1.961
8500	Y = 10.216 X – 14.119
9000	Y = 1.782 X – 2.153
9500	Y = 4.773 X – 6.644

Table 3. Values of β with confidence intervals

Aging Time (h)	Shape Parameter
0	9.595 < β = 11.985 < 14.150
500	4.619 < β = 5.769 < 6.811
1000	1.698 < β = 2.121 < 2.504
1500	1.688 < β = 2.108 < 2.489
2000	1.797 < β = 2.244 < 2.649
2500	4.062 < β = 5.074 < 5.991
3000	5.660 < β = 7.070 < 8.347
3500	5.121 < β = 6.397 < 7.553
4000	4.600 < β = 5.746 < 6.784
4500	4.772 < β = 5.960 < 7.037
5000	1.297 < β = 1.620 < 1.913
5500	4.876 < β = 6.090 < 7.190
6000	8.963 < β = 11.195 < 13.217
6500	5.187 < β =6.479 < 7.649
7000	8.182 < β = 10.221 < 12.066
7500	8.101 < β =10.118 < 11.946
8000	1.342 < β = 1.676 < 1.979
8500	8.179 < β = 10.216 < 12.062
9000	1.427 < β = 1.782 < 2.104
9500	3.821 < β = 4.773 < 5.635

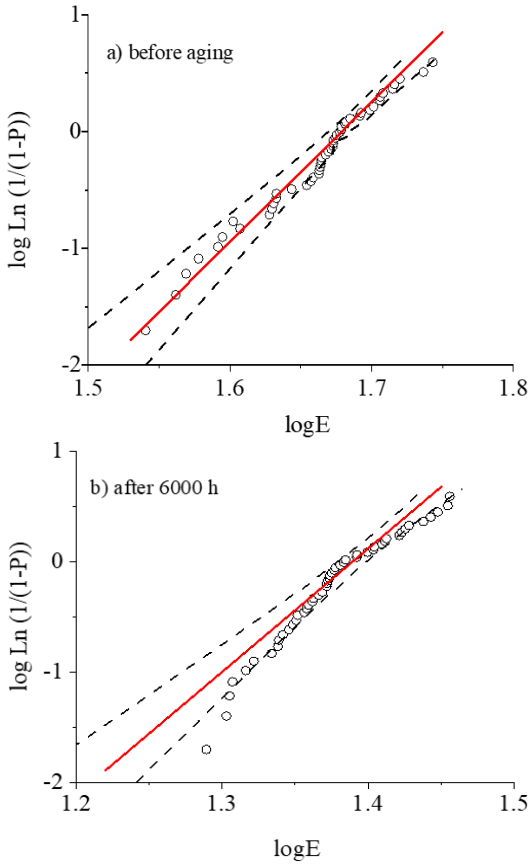

Figure 1. Weibull plots of dielectric strength before aging and after 6000 h

4.1.2 Variation of dielectric strength versus aging time

The variation of dielectric strength in a function of aging time is exhibited in Figure 2. The changes can be depicted as follows:

•At the beginning, E drops from 47.74 kV/mm to 8.15 kV/mm and increases rapidly until 28.02 kV/mm corresponding to 2500 h.

•Afterwards E lessens to 24.88 kV/mm, enlarges up to 31.29 kV/mm, and then falls to 7.19 kV/mm after 5000 h.

•After this time, E rises rapidly to 24.59 kV/mm for 5500 h. Then it enhances slowly to 27.57 kV/mm and shortens until 25.39 kV/mm corresponding to 7500 h.

•Latter E weakens to 14.80 kV/mm and grows to 24.11 kV/mm for 8500 h. Beyond this time, it lowers to 16.17 kV/mm and augments again until 24.66 kV/mm for an aging time of 9500 h. The maximum variation is 84.94%.

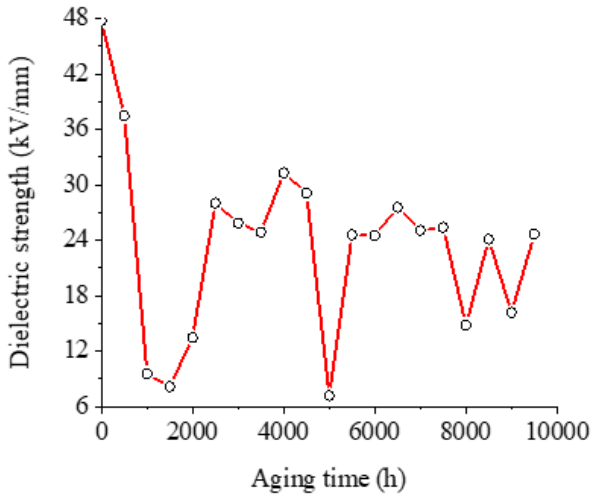

Figure 2. Dielectric strength against aging time

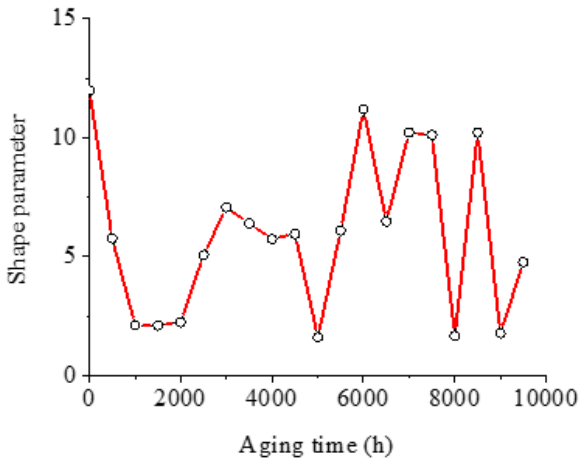

Figure 3. Shape parameter of dielectric strength against aging time

4.1.3 Change of shape parameter against aging time

Figure 3 displays the dependence of aging time on the shape parameter for dielectric strength. The variations of β can be described as follows:

•At the first, β decreases abruptly from 11.99 to 2.12 and remains somewhat invariable until 2000 h. Afterwards β grows to 7.07 and lowers to 5.75, and becomes practically constant until 4500 h.

•Beyond this time, it lessens to 1.62 and grows rapidly to 11.20 and shortens again up to 6.48 for 6500 h. Latter β rises over 10.22 and stays constant until 7500 h.

•After, β falls to 1.68 and rises quickly to 10.22 for 8500 h. Then it decays to 1.78 and heightens again to 4.77 for 9500 h. The maximum variation is 86.49%.

4.2 Elongation at break

4.2.1 Weibull graphs

The statistical results of elongation at break (ε) are presented in Tables 4-6. Figure 4 shows Weibull graphs of ε before aging and after 6000 h.

Table 4. Values of elongation at break and confidence intervals

Aging Time (h)	Elongation at Break (%)
0	5.227 < ε = 5.432 < 5.634
500	9.249 < ε = 9.540 < 9.825
1000	9.785 < ε = 10.128 < 10.464
1500	9.560 < ε = 9.911 < 10.255
2000	9.113 < ε = 9.425 < 9.730
2500	6.898 < ε = 7.315 < 7.733
3000	8.449 < ε = 8.747 < 9.040
3500	8.894 < ε = 9.224 < 9.548
4000	7.992 < ε = 8.269 < 8.540
4500	7.746 < ε = 8.009 < 8.266
5000	9.620 < ε = 9.894 < 10.161
5500	7.662 < ε = 7.981 < 8.296
6000	9.409 < ε = 9.693 < 9.970
6500	8.104 < ε = 8.367 < 8.624
7000	8.348 < ε = 8.618 < 8.882
7500	8.680 < ε = 9.003 < 9.321
8000	8.990 < ε = 9.255 < 9.513
8500	8.781< ε = 9.062<9.337
9000	8.837< ε = 9.131<9.419
9500	8.734 < ε = 9.094 < 9.463

Table 5. Equation of Weibull plots

Aging Time (h)	Equation of Weibull Plot
0	Y = 6.741 X – 4.955
500	Y = 8.359 X – 8.188
1000	Y = 7.520 X – 7.561
1500	Y = 7.191 X – 7.163
2000	Y = 7.708 X – 7.510
2500	Y = 4.416 X – 3.817
3000	Y = 7.462 X – 7.028
3500	Y = 7.118 X – 6.869
4000	Y = 7.607 X – 6.979
4500	Y = 7.773 X – 7.024
5000	Y = 9.226 X – 9.183
5500	Y = 6.354 X – 5.731
6000	Y = 8.723 X – 8.605
6500	Y = 8.117 X – 7.488
7000	Y = 8.142 X – 7.616
7500	Y = 7.085 X – 6.762
8000	Y = 8.922 X – 8.622
8500	Y = 8.211 X – 7.860
9000	Y = 7.918 X – 7.606
9500	Y = 6.231 X – 5.974

Table 6. Values of β with confidence intervals

Aging Time (h)	Shape Parameter
0	5.397 < β = 6.741 < 7.959
500	6.692 < β = 8.359 < 9.869
1000	6.021 < β = 7.520 < 8.878
1500	5.757 < β = 7.191 < 8.490
2000	6.171 < β = 7.708 < 9.100
2500	3.535 < β = 4.416 < 5.214
3000	5.974 < β = 7.462 < 8.810
3500	5.699 < β = 7.118 < 8.404
4000	6.090 < β = 7.607 < 8.981
4500	6.223 < β = 7.773 < 9.177
5000	7.386 < β = 9.226 < 10.893
5500	5.087 < β = 6.354 < 7.502
6000	6.984 < β = 8.723 < 10.299
6500	6.499 < β =8.117 < 9.583
7000	6.519 < β = 8.142 < 9.613
7500	5.672 < β =7.085 < 8.365
8000	7.143 < β = 8.922 < 10.534
8500	6.574 < β = 8.211 < 9.694
9000	6.339 < β = 7.918 < 9.348
9500	5.023 < β = 6.231 < 7.334

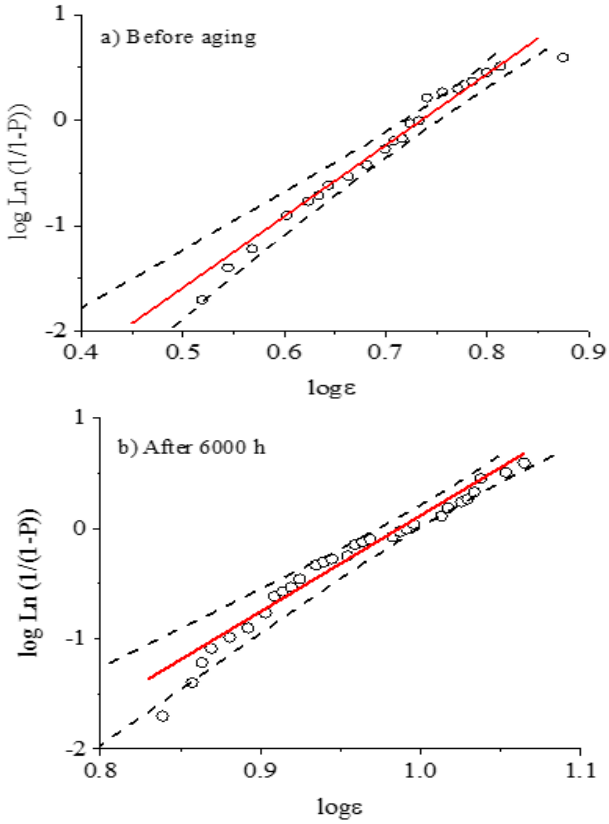

Figure 4. Weibull plots of elongation at the break before aging and after 6000 h

4.2.2 Variation of elongation at break versus aging time

Figure 5 shows the variation of elongation at break versus aging time. The changes can be summed as follows:

•During the first 1000 h of aging, ε increases quickly from 5.43% to 10.13% and decays to 7.32% after 2500 h.

•Beyond this time, ε rises to 9.22% and decreases until 8.01, then grows again to 9.89% for 5000 h.

•After 5000 h, the elongation at break lessens to 7.98%, raises to 9.69%, and shortens to 8.37% for 6500 h.

•Afterwards, ε enhances slowly to 9.26% then lowers slightly until 9.06% and stays somewhat invariable up to 9500 h. The maximum change is 86.56%.

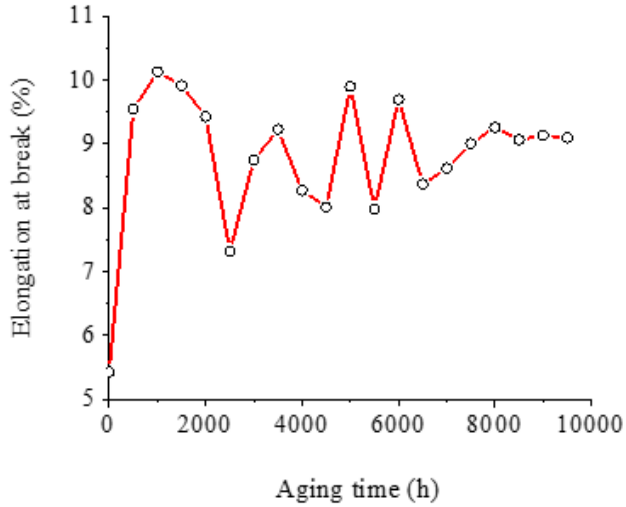

Figure 5. Elongation at the break in the function of aging time

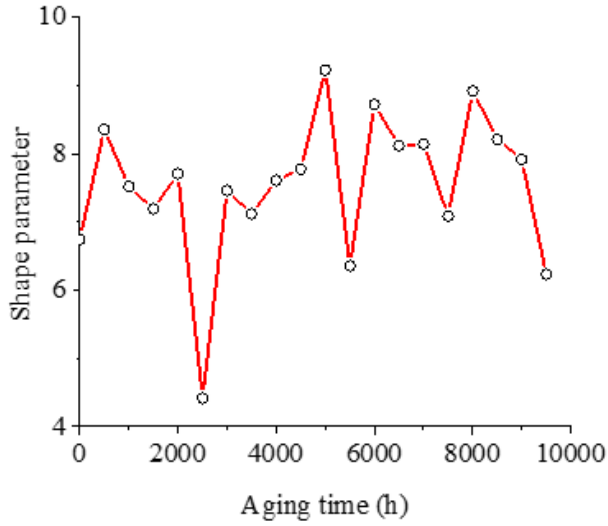

Figure 6. Shape parameter of elongation at break against aging time

4.2.3 Changing of shape parameter in the function of aging time

Figure 6 presents the shape parameter for elongation at break versus aging time. The changes can be resumed as follows:

•At first, β increases from 6.74 to 8.36, lowers to 7.19, and augments again, reaching 7.71 for 2000 h.

•After this time, β falls to 4.41, enlarges quickly to 7.48, and lessens to 7.12 after 3500 h.

•Afterwards it grows to 9.23, drops until 6.34, and increases rapidly to 8.72 corresponding to 6000 h.

•Later, β decays to 7.09, rises up to 8.92, and weakens speedily to 6.23 for 9500 h. The maximum variation is 36.94%.

4.3 Tensile strength

4.3.1 Weibull graphs

The statistical findings of tensile strength (σ) are displayed in Tables 7-9. Figure 7 exposes the Weibull graphs of σ before and after 6000 h.

Table 7. Values of Ϭ and confidence intervals

Aging Time (h)	Tensile (MPa)
0	222.443 < Ϭ = 231.382 < 240.185
500	176.789 < Ϭ = 182.498 < 188.065
1000	155.554 < Ϭ = 160.410 < 165.154
1500	108.929 < Ϭ = 113.422 < 117.849
2000	170.256 < Ϭ = 176.509 < 182.632
2500	181.623 < Ϭ = 190.243 < 198.788
3000	188.475 < Ϭ = 195.881 < 203.170
3500	173.703< Ϭ = 179.248 < 184.653
4000	192.671 < Ϭ = 201.32 < 209.879
4500	181.258 < Ϭ = 191.117 < 200.945
5000	147.883 < Ϭ = 154.153 < 160.337
5500	176.592 < Ϭ = 183.422 < 190.138
6000	148.731 < Ϭ = 153.363 < 157.882
6500	169.647 < Ϭ = 180.165 < 190.729
7000	175.444 < Ϭ = 181.801 < 188.039
7500	168.188 < Ϭ = 175.113 < 181.936
8000	141.269 < Ϭ = 146.461 < 151.558
8500	153.985< Ϭ = 159.147<164.187
9000	154.202 < Ϭ = 162.501 < 170.780
9500	88.350 < Ϭ = 92.792 < 97.209

Table 8. Equation of Weibull graphs

Aging Time (h)	Equation of Weibull Plot
0	Y = 6.577 X – 15.551
500	Y = 8.163 X – 18.406
1000	Y = 8.429 X – 18.587
1500	Y = 6.413 X – 13.177
2000	Y = 7.193 X – 16.162
2500	Y = 5.589 X – 12.740
3000	Y = 6.723 X – 15.410
3500	Y = 8.257 X – 18.607
4000	Y = 5.900 X – 13.592
4500	Y = 4.895 X – 11.168
5000	Y = 6.242 X – 13.657
5500	Y = 6.829 X – 15.457
6000	Y = 8.453 X – 18.477
6500	Y = 4.309 X – 9.719
7000	Y = 7.280 X – 16.451
7500	Y = 6.424 X – 14.411
8000	Y = 7.179 X – 15.547
8500	Y = 7.868 X – 17.324
9000	Y = 4.943 X – 10.929
9500	Y = 5.282 X – 10.392

Table 9. Values of β with confidence intervals

Aging Time (h)	Shape Parameter
0	5.266 < β = 6.577 < 7.765
500	6.535 < β = 8.163 < 9.638
1000	6.748 < β = 8.429 < 9.952
1500	5.134 < β = 6.413 < 7.572
2000	5.759 < β = 7.193 < 8.492
2500	4.475 < β = 5.589 < 6.599
3000	5.382 < β = 6.723 < 7.938
3500	6.611 < β = 8.257 < 9.749
4000	4.724 < β = 5.900 < 6.966
4500	3.919 < β = 4.895 < 5.779
5000	4.997 < β = 6.242 < 7.370
5500	5.467 < β = 6.829 < 8.063
6000	6.768 < β = 8.453 < 9.980
6500	3.450 < β =4.309 < 5.087
7000	5.828 < β = 7.280 < 8.595
7500	5.143 < β =6.424 < 7.584
8000	5.748 < β = 7.179 < 8.476
8500	6.299 < β = 7.868 < 9.289
9000	3.957 < β = 4.943 < 5.836
9500	4.229 < β = 5.282 < 6.236

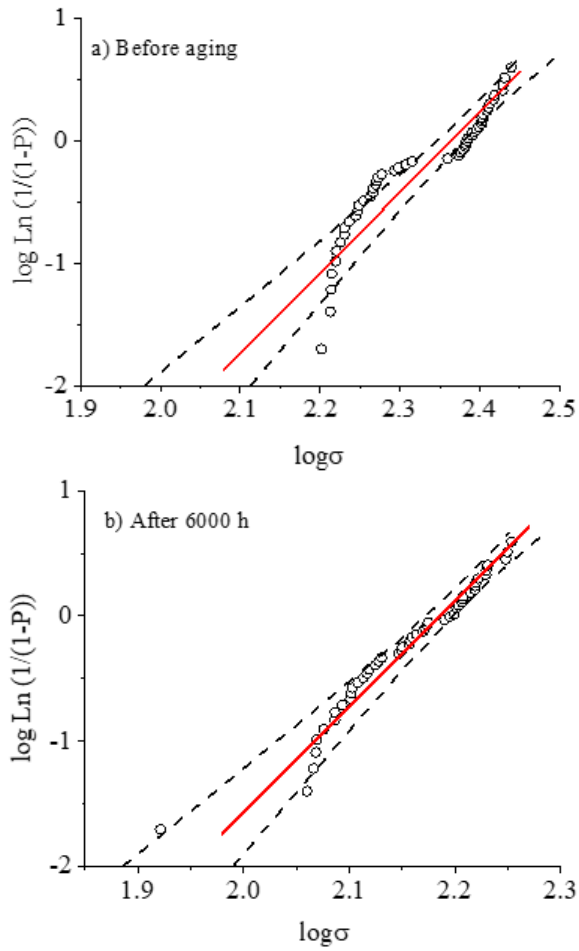

Figure 7. Weibull plots of tensile strength before aging and after 6000 h

4.3.2 Dependence of aging time on tensile strength

Figure 8 shows the variation of tensile strength versus aging. The changes can be summarized as follows:

•Firstly, Ϭ drops from 231.38 MPa to 113.42 MPa and raises to 195.88 MPa after 3000 h. Then it decreases a little to 179.25 MPa and grows again until 201.32 MPa for 4000 h.

•Afterwards, Ϭ lowers to 154.15 MPa, increases to 183.42 MPa, and diminishes again to 153.36 MPa after 6000 h

•Beyond this time, Ϭ raises to 181.80 MPa and shortens to 146.46 MPa for 8000 h. After Ϭ augments slightly over 162.50 MPa and falls to 92.79 MPa after 9500 h. The maximum variation is 59.90%.

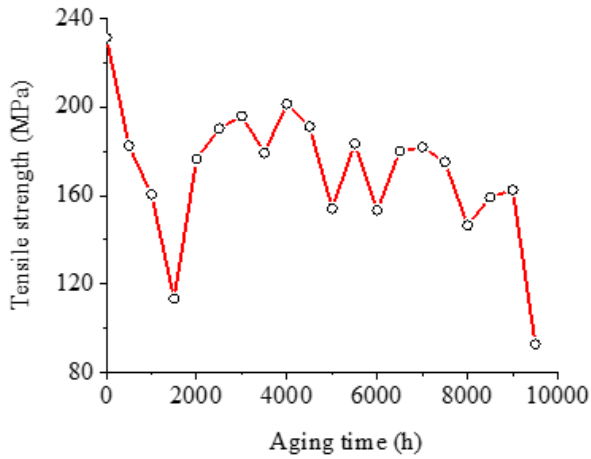

Figure 8. Tensile strength against aging time

4.3.3 Changing of shape parameter in the function of aging time

Figure 9 presents the dependence of aging on the shape parameter for tensile strength. The evolution is resumed below:

•At the beginning, β increases from 6.58 to 8.43, lowers till 6.41 then augments back attaining 7.19 after 2000 h. Belong 2000 h, β weakens to 5.59, grows quickly reaching 8.26, and decays to 4.90 after 4500 h.

•Afterwards β increases rapidly to 8.45, drops to 4.31, and raises speedily until 7.28 after 7000 h.

•Later, β lowers to 6.42, raises up to 7.87, and falls to 4.94 then it increases a little to 5.28 after 9500 h. The maximum change is 34.50%.

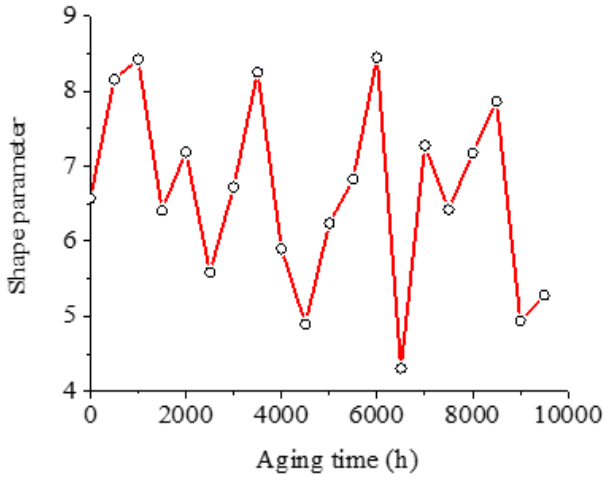

Figure 9. Shape parameter of tensile strength versus aging time

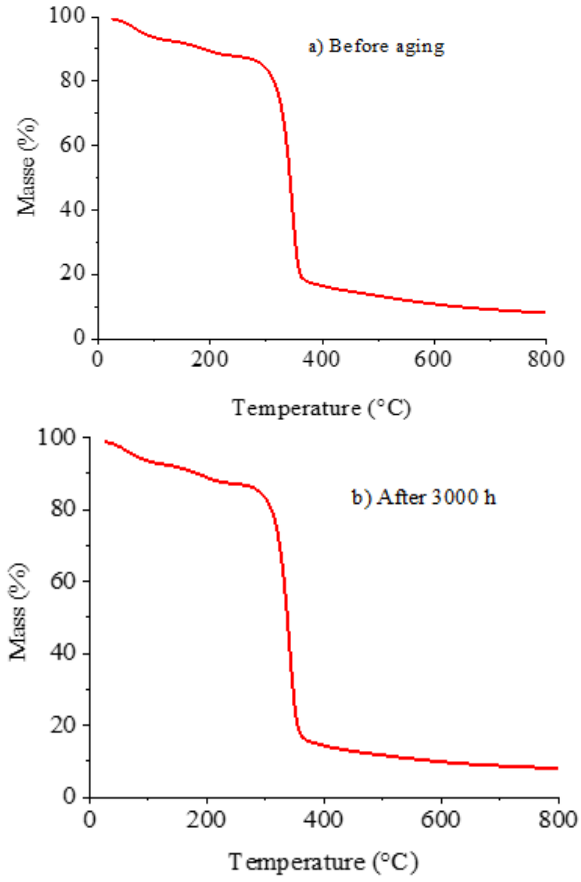

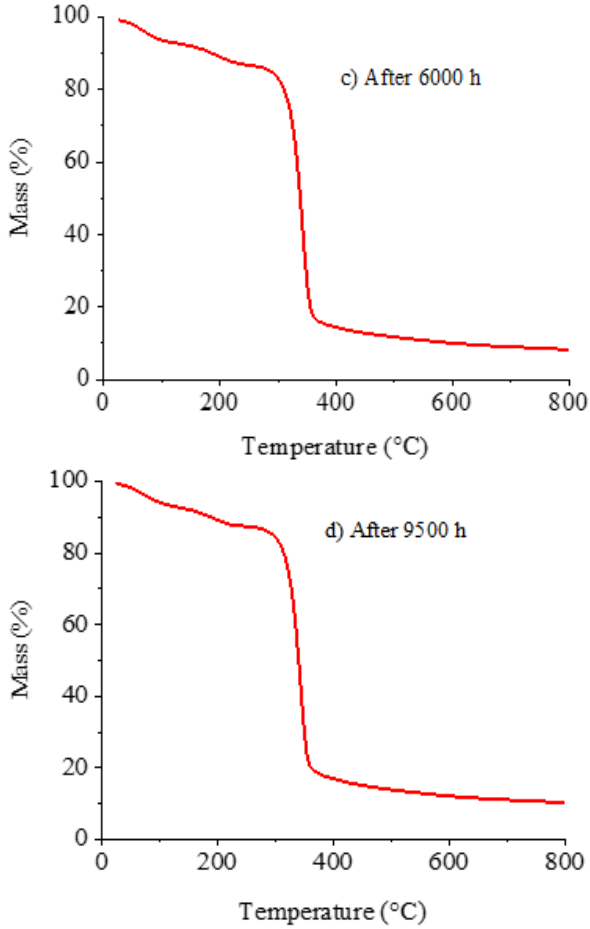

Figure 10. Thermogravimetric curves

4.4 TGA

The thermogravimetric curves are exposed in Figure 10. As it can be seen, these curves have the same form. The evolutions are summarized below.

•Between 26°C and 320°C, a decrease of about 17.3% in the mass is noticed before and after aging. This lessening is attributed to the evaporation of water and volatile solvents.

•Before aging, the mass loss begins at about 318°C, accelerates and reaches 85.1% at 362°C. Then it slackens and it remains a residue of 7.50% at 799°C. The temperature corresponding to 50% mass loss is 338°C.

•After 3000 h, the mass loss initiates at about 323°C. Beyond the onset temperature, it expedites and achieves 87.6% at 350°C. After, the mass loss decelerates and it stays a residue of 7.9% at 799°C. The 50% mass loss is reached at 338°C.

•After 6000 h, the mass loss begins at around 325°C and quickens up to 87.4% at about 350°C. Next, the mass loss goes slow and it remains a residue of 8% at 799°C. The 50% mass loss is attained at 337°C.

•After 9500 h, the mass loss starts at 321°C and hastens to 85.4% at about 365°C. Later, it slows down leading to a remainder of 10% at 799°C. The temperature matching to 50% mass loss is 341°C.

4.5 FTIR

In Table 10, the significant infrared absorbance bands of oil-impregnated pressboard are presented.

Table 10. Absorbance bands

Absorbance Band Number	Wavenumber (cm^{-1})
1	3344
2	2917
3	2858
4	1653
5	1455
6	1044

From Figure 11, we can observe the following details.

Before aging:

•It appears an absorbance band at 3344 cm^{-1} allotted to the stretching vibrations of hydroxyl groups (OH) [18, 19].

•We notice two absorbance peaks at 2917 and 2858 cm^{-1} attributed to the stretching vibration of C-H groups [18].

•The absorbance peak, detected at 1653 cm^{-1}, matches to the carbonyl compound associated with cellulose [18].

•We observe an absorbance peak at 1455 cm^{-1} which highlights the presence of the aromatic compound fingerprints [20, 21].

•It arises an absorbance peak at 1044 cm^{-1} corresponding to the C-O valence vibration [18].

After aging, we note alterations in the spectra:

•After 3000 h, we notice an increase in the intensities of the absorbance peaks at 3344 and 1044 cm^{-1}.

•After 6000 h, the intensities of the absorbance peaks at 3344 and 2917 cm^{-1} drop as it can be shown in the spectrum.

•After 9500 h, it is clear that the intensity of the absorbance peak at 3344 cm^{-1} decreases. So, we show that the intensity of the absorbance peak at 2917 cm^{-1} heightens. On the other hand, the absorbance peak at 1653 cm^{-1} disappeared.

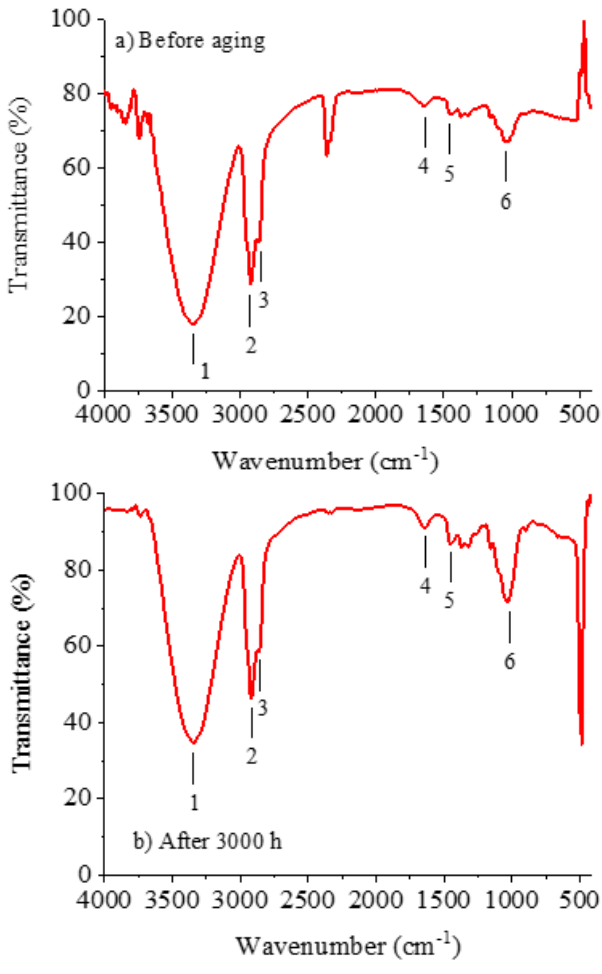

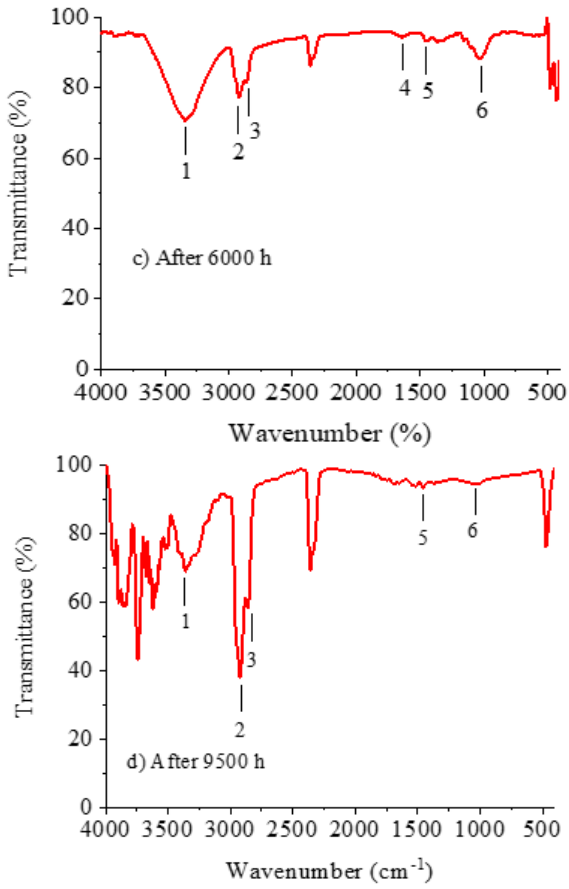

Figure 11. FTIR spectra

4.6 Discussion

At long term, water can diffuse through the amorphous regions of the insulating material as yielded by Holdge et al. [22]. The cristalline regions are considered impermeable. The absorbed water transforms the polymer more polar as related by Van Krevelen and Nijenhuis [23].

The hydrolytic aging shortens the viscosity of the dielectric material expressing a reduction of molecular bonds and an increase in free volume. Therefore, the mean free path and the mobility of charge carriers grow leading to the decrease of the dielectric strength. While the increase of the dielectric strength can be explained by the arrangement in the structure producing, in the contrary, a decrease in the mean free path and the mobility of charge carriers.

Dielectric strength is related to the presence of defects which can be voids, electrode asperities and laminations at the electrode-polymer interface. These defects can exist within the insulation during the manufacturing or created over the hydrolytic aging. During the dielectric testing, electrical tree or water tree initiates from the defects and propagates leading to breakdown. The phenomena were described elsewhere [24]. Martin et al. [25] reported that the relative permittivity of the oil is about 2.2. While the relative permittivity of impregnated pressboard is 4.4. When a voltage is applied to oil-impregnated pressboard, the electric stress is more important in the oil. When the electric field reaches a certain level, electrical discharges occur in the oil and damage the pressboard by dielectric failure.

Elongation at break and tensile strength vary in function of aging time. This process can be explained by the fact that the diffusion of water causes a plasticization of the insulation.

This phenomenon has been yielded by Merdas et al. [26]. After some aging time, the arrangement of the molecular structure of the material can take place. From Figure 8, we determined the lifetime-end of the material which is 9348 h. The criterion of lifetime-end was chosen for a 50% loss of the tensile strength.

The shape parameter measures the dispersion of the values of the properties. As one can see, the shape parameter of data alters from one distribution to another. This change is assigned to the size distribution and the type of defects. This result has been reported in a previous work [27].

After aging, modifications of the thermogravimetric curves are shown:

•The onset temperature of the decomposition varies between 318°C and 325°C.

•The final temperature of degradation differs from 350°C to 365°C.

•The residue alters between 7.5% and 10%.

According to TGA curves, we conclude that the decomposition of the insulation is done in one step: The process is governed by a first-order chemical reaction.

Hydrolysis of oil produces acids, and carbon dioxide, increases acidity of insulation oil, reduces interfacial tension, and leads to sludging of oil. Hydrolysis of insulation paper tends to lower the degree of polymerisation of paper, increase dissolved decay contents, form soluble sludge, increase viscosity, and contaminate the insulation oil [28]. Hydrolysis of cellulose paper is catalysed by H+ ions which are derived by the dissociation of carboxyl acid in water [29] and thereby aging process in paper insulation is affected due to both moisture and acids [29, 30].

The degradation was characterized by a decrease in the degree of polymerization of the pressboard and the formation of both 2-furfuraldehyde and dissolved carbon dioxide (CO_2) in the oil [18]. A change in the color of the insulation, from yellow to brown, was shown after aging.

Degradation involves the breaking of covalent bonds within and between monomer units in the chain and the loss of inter- and intra-chain hydrogen bonds as reported by Emsley and Stevens [31].

5. CONCLUSIONS

This investigation allows deducting the following points:

•Dielectric strength, elongation at break, and strength tensile are altered by hydrolytic aging.

•During aging, water can penetrate into the material. This phenomenon leads to the plasticization of the insulating material inducing a change of the properties. Afterwards, the rearrangement in the structure of the dielectric material can occur.

-After aging, the physico-chemical tests highlight the degradation of the polymer. TGA indicates modifications of onset temperature and the residue of decomposition.

-FTIR analysis shows alteration of the absorbance peaks at 3344, 2917, and 1044 cm^{-1}. Further, it was observed a vanishing of the absorbance peak at 1653 cm^{-1}.

•The decomposition of the insulation is done according to one stage: The process is ruled by a first-order chemical reaction.

•After aging, the colour of the insulating material changed from yellow to brown.

•Future studies can be executed:

-Effect of hydrolytic aging on the properties of oil-impregnated pressboard at 40°C under different moisture quantities: 30%, 40%, 50%, 60%, 70%, 80%. This investigation will permit deducting characteristics giving a lifetime of insulation versus moisture amount.

-Influence of hydrothermal aging on the properties of oil-impregnated pressboard at 100°C and 93% relative moisture amount. The results will be compared with those of this investigation.

-The oil-impregnated pressboard will be characterized by TGA and FTIR.

REFERENCES

[1] Gao, C., Qi, B., Li, C., Lu, L., Zhang, S. (2019). Key dielectric properties and performance evaluation of high-density pressboard for electrical purposes. AIP Advances, 9(11): 115317. https://doi.org/10.1063/1.5125308

[2] Oommen, T.V., Prevost, T.A. (2006). Cellulose insulation in oil-filled power transformers: Part II-Maintaining insulation integrity and life. IEEE Electrical Insulation Magazine, 22(2): 5-14. https://doi.org/10.1109/MEI.2006.1618996

[3] Dai, J., Wang, Z.D. (2008). A comparison of the impregnation of cellulose insulation by ester and mineral oil. IEEE Transactions on Dielectrics and Electrical Insulation, 15(2): 374-381. https://doi.org/10.1109/TDEI.2008.4483455

[4] Wen, H., Cheng, L., Jiang, Y., Zhao, Z., Ye, W., Hao, J. (2020). Experimental and simulation analysis of the influence of moisture on dielectric and breakdown properties of insulation pressboard used in power transformer. Journal of Physics: Conference Series, 1678(1): 012047. https://doi.org/10.1088/1742-6596/1678/1/012047

[5] Vahidi, F., Tenbohlen, S., Roesner, M., Perrier, C., Stirl, T. (2015). The influence of the moisture during the electrical conductivity measurement on impregnated high density pressboard. In the 19th International Symposium on High Voltage Engineering, Pilsen, Czech Republic, pp. 1035-1040.

[6] Wang, H., Yang, Y., Li, C.R., Zheng, Z., Jia, J.J. (2010) Influence of micro water on partial discharge between windings in transformers. Gaodianya Jishu/High Voltage Engineering, 36(5): 1143-1149.

[7] Emsley, A.M., Stevens, G.C. (1992). A reassessment of the low temperature thermal degradation of cellulose. In Sixth International Conference on Dielectric Materials, Measurements and Applications, Manchester, UK, pp. 229-232.

[8] Jadav, R.B., Ekanayake, C., Saha, T.K. (2014) Understanding the impact of moisture and ageing of transformer insulation on frequency domain spectroscopy. IEEE Transactions on Dielectrics and Electrical Insulation, 21(1): 369-379. https://doi.org/10.1109/TDEI.2013.003984

[9] Khawaja, R.H., Ariastina, W.G., Blackburn, T.R. (2003). Partial discharge behaviour in oil-impregnated insulation. In 7th International Conference on Properties and Applications of Dielectric Materials, Nagoya, pp. 1166-1169. https://doi.org/10.1109/ICPADM.2003.1218631

[10] Kumar, A., Haque, N. (2023). Effect of ageing and moisture on dielectric properties of natural ester impregnated pressboard insulation. In 2023 5th International Conference on Energy, Power and Environment: Towards Flexible Green Energy Technologies (ICEPE), Shillong, India, pp. 1-5. https://doi.org/10.1109/ICEPE57949.2023.10201619
[11] IEC 60540. (1982). Test methods for insulations and sheaths of electric cables and cords (elastomeric and thermoplastic compounds). https://webstore.iec.ch/en/publication/16539.
[12] Weibull, W. (1951). A statistical distribution function of wide applicability. Journal of Applied Mechanics, 18: 293-297. https://doi.org/10.1115/1.4010337
[13] Nedjar, M. (2011). Investigation in thermal endurance of polyesterimide used in electrical machines. Journal of Applied Polymer Science, 121(5): 2886-2892. https://doi.org/10.1002/app.33904
[14] Kerkarine, F., Nedjar, M. (2024). Hydrolytic aging of wire enameled with polyesterimide and polyamide imide used in electrical machines. Mathematical Modelling of Engineering Problems, 11(4): 1053-1059. https://doi.org/10.18280/mmep.110423
[15] Diaham, S., Zelmat, S., Locatelli, M., Dinculescu, S., Decup, M., Lebey, T. (2010). Dielectric breakdown of polyimide films: Area, thickness and temperature dependence. IEEE Transactions on Dielectrics and Electrical Insulation, 17(1): 18-27. https://doi.org/10.1109/TDEI.2010.5411997
[16] Chauvet, C., Laurent, C. (1993). Weibull statistics in short-term dielectric breakdown of thin polyethylene films. IEEE Transactions on Electrical Insulation, 28(1): 18-29. https://doi.org/10.1109/14.192236
[17] Raju, G., Katebian, A., Jafri S.Z. (2001). Application of Weibull distribution for high temperature breakdown data. In 2001 Annual Report Conference on Electrical Insulation and Dielectric Phenomena (Cat. No.01CH37225), Kitchener, ON, Canada, pp. 173-176. https://doi.org/10.1109/CEIDP.2001.963514
[18] Bandara, K., Ekanayake C., Saha, T.K., Kumar Annamalai, P. (2016). Understanding the ageing aspects of natural ester based insulation liquid in power transformer. IEEE Transactions on Dielectrics and Electrical Insulation, 23(1): 246-257. https://doi.org/10.1109/TDEI.2015.004744
[19] Liu, C., Zhang, W., Xu, M., Shi, L., Zhao, Y. (2016). A study of aging property of pressboard in gas insulator transformer. In 2016 IEEE International Conference on Dielectrics (ICD), Montpellier, France, pp. 772-775. https://doi.org/10.1109/ICD.2016.7547730
[20] Fofana, I., Bouaicha, A., Farzaneh, M. (2011). Characterization of aging transformer oil-pressboard insulation using some modern diagnostic techniques. European Transactions on Electrical Power, 21(1): 1110-1127. https://doi.org/10.1002/etep.499
[21] Sarathi, R., Sheema, I.M., Rajan, J.S. (2014). Understanding surface discharge activity in copper sulphide diffused oil impregnated pressboard under AC voltages. IEEE Transactions on Dielectrics and Electrical Insulation, 21(2): 674-682. https://doi.org/10.1109/TDEI.2013.004039
[22] Hodge, R.M., Edward, G.H., Simon, G.P. (1996). Water absorption and states of water in semicrystalline poly (vinyl alcohol) films. Polymer, 37(8): 1371-1376. https://doi.org/10.1016/0032-3861(96)81134-7
[23] Van Krevelen, D.W., Nijenhuis, K.T. (2009). Properties of Polymers. Elsevier.
[24] Dissado, L.A., Fothergill, J.C. (1992). Electrical Degradation and Breakdown in Polymers. Peter Peregrinus.
[25] Martin, D., Wang, Z.D., Dyer, P., Darwin, A.W., James, I.R. (2007). A comparative study of the dielectric strength of ester impregnated cellulose for use in large power transformers. In 2007 IEEE International Conference on Solid Dielectrics, Winchester, UK, pp. 294-297. https://doi.org/10.1109/ICSD.2007.4290810
[26] Merdas, I., Thominette, F., Verdu, J. (2000). Humid aging of polyetherimide. II. Consequences of water absorption on thermomechanical properties. Journal of Applied Polymer Science, 77(7): 1445-1451. https://doi.org/10.1002/1097-4628(20000815)77:7%3C1445::AID-APP6%3E3.0.CO;2-N
[27] Nedjar M., Kerkarine F. (2024). Weibull statistic in hydrolytic aging of polyesterimide used in rotating electrical machine windings. Mathematical Modelling of Engineering Problems, 11(10): 2740-2748. https://doi.org/10.18280/mmep.111016
[28] Moore, S., Rapp, K., Baldyga, R. (2012). Transformer insulation dry out as a result of retrofilling with natural ester fluid. In PES T&D 2012, Orlando, FL, USA, pp. 1-6. https://doi.org/10.1109/TDC.2012.6281441
[29] Lundgaard, L.E., Hansen, W., Ingebrigten, S. (2008). Ageing of mineral oil-impregnated cellulose by acids catalysis. IEEE Transactions on Dielectrics and Electrical Insulation, 15(2): 540-546. https://doi.org/10.1109/TDEI.2008.4483475
[30] Lundgaard, L.E., Hansen, W., Linhjell, D., Painter, T.J. (2004). Aging of oil-impregnated paper in power transformers. IEEE Transactions on Power Delivery, 19(1): 230-239. https://doi.org/10.1109/TPWRD.2003.820175
[31] Emsley, A.M., Stevens, G.C. (1994). Kinetics and mechanisms of the low temperatures degradation of cellulose. Cellulose, 1: 26-56. https://doi.org/10.1007/BF00818797